

# Journal of Biomedical Optics

BiomedicalOptics.SPIEDigitalLibrary.org

## **Identification of individual biofilm-forming bacterial cells using Raman tweezers**

Ota Samek  
Silvie Bernatová  
Jan Ježek  
Martin Šiler  
Mojmir Šerý  
Vladislav Krzyžánek  
Kamila Hrubanová  
Pavel Zemánek  
Veronika Holá  
Filip Růžička

# Identification of individual biofilm-forming bacterial cells using Raman tweezers

Ota Samek,<sup>a,\*</sup> Silvie Bernatová,<sup>a</sup> Jan Ježek,<sup>a</sup> Martin Šiler,<sup>a</sup> Mojmir Šerý,<sup>a</sup> Vladislav Krzyžánek,<sup>a</sup> Kamila Hrubanová,<sup>a</sup> Pavel Zemánek,<sup>a</sup> Veronika Holá,<sup>b</sup> and Filip Růžička<sup>b</sup>

<sup>a</sup>Institute of Scientific Instruments of the AS CR, v.v.i., Královopolská 147, 612 64 Brno, Czech Republic

<sup>b</sup>Masaryk University and St. Anne's Faculty Hospital, Department of Microbiology, Faculty of Medicine, Pekařská 53, 656 91 Brno, Czech Republic

**Abstract.** A method for *in vitro* identification of individual bacterial cells is presented. The method is based on a combination of optical tweezers for spatial trapping of individual bacterial cells and Raman microspectroscopy for acquisition of spectral “Raman fingerprints” obtained from the trapped cell. Here, Raman spectra were taken from the biofilm-forming cells without the influence of an extracellular matrix and were compared with biofilm-negative cells. Results of principal component analyses of Raman spectra enabled us to distinguish between the two strains of *Staphylococcus epidermidis*. Thus, we propose that Raman tweezers can become the technique of choice for a clearer understanding of the processes involved in bacterial biofilms which constitute a highly privileged way of life for bacteria, protected from the external environment. © 2015 Society of Photo-Optical Instrumentation Engineers (SPIE) [DOI: 10.1117/1.JBO.20.5.051038]

Keywords: Raman tweezers; *Staphylococcus epidermidis*; biofilm.

Paper 140661SSR received Oct. 9, 2014; accepted for publication Feb. 5, 2015; published online Mar. 2, 2015.

## 1 Introduction

Many microorganisms (e.g., bacteria, yeast, and algae) are known to form a multilayered structure composed of cells and extracellular matrix on various types of surfaces. Such a formation is known as the biofilm.<sup>1–5</sup> Special attention is now paid to bacterial biofilms that are formed on the surface of medical implants, surgical fixations, and artificial tissue/vascular replacements. Cells contained within such a biofilm are well protected against antibiotics and phagocytosis and, thus, effectively resist antimicrobial attack. Microbial infections resulting from the biofilm formation represent a serious complication in the treatment of open fractures, cardiovascular diseases, and organ transplants.<sup>1–3</sup> Elucidation of the basic mechanisms of the biofilm formation would contribute to deeper understanding of the basic biochemical mechanisms underlying this process and developing new and more efficient strategies for the infection treatment or even protection.

*Staphylococcus epidermidis* represents one of the most virulent bacteria, mainly attributed to its surface colonization and biofilm formation in medicine. A biofilm represents an adherent, structured, high density community of bacterial cells embedded in an extracellular matrix, previously called slime<sup>2</sup> (Fig. 1). Polysaccharide intracellular adhesion (PIA) is considered as the major functional component contained in the extracellular matrix which mediates the intercellular adhesion and thus formation of *S. epidermidis* biofilms.

The chemical analysis of an extracellular matrix reveals a range of macromolecules, including carbohydrates, carbohydrate containing proteins, and/or peptidoglycans. For example, Karamanos et al.<sup>5</sup> identified the following constituents: protein (19% to 26%), amino sugars (10% to 31%), neutral sugars (4% to 16%), hexuronic acid (3% to 13%), esterified phosphates (7% to 12%), and total sulfates (2% to 4%). A key component of

the extracellular matrix in *S. epidermidis* biofilm is poly-N-acetylglucosamine, the linear homopolymer N-acetylglucosamine linked with a  $\beta$ -1,6-glycosidic linkage whose subunits are randomly deacetylated, enabling the aggregation of staphylococcal cells and thus also facilitating accumulation in biofilm.<sup>3</sup> However, all of them exhibit a wide spread in relative composition within the given sample.

When characterizing biofilms using spectroscopic techniques, and specifically Raman spectroscopy, a common approach is to analyze biofilm as a whole (cells embedded in extracellular matrix). Such spectra were acquired point-by-point at selected positions of individual colonies or using line-scan techniques such as, e.g., Renishaw StreamLine.<sup>6,7</sup>

Beier et al. studied the identification of different bacteria in biofilms using confocal Raman spectroscopy.<sup>8</sup> In this study, the sample volume size was larger than a single bacterium so that some extracellular polysaccharides (EPS) could be present in the Raman sampling volume along with the cells. It was found that, in principle, the source of species-specific spectral signatures could be the EPS rather than the bacterial cells themselves. Moreover, McEwen et al. investigated the characteristic Raman peaks which could be beneficial to evaluate the presence or absence of particular EPS components developed on KT2440 cell surface during different culture times.<sup>9</sup> It was concluded that Raman microspectroscopy was able to identify biochemical structural components of bacterial EPS versus culture time. Thus, the just mentioned approach collects data from many cells including the contribution from extracellular matrix. Note that in most biofilms, the microorganisms account for less than 10% of the dry mass, whereas the extracellular matrix can account for over 90%.<sup>10</sup>

Therefore, when measuring only the “clean” single cell contributions, there is a lack of specificity, which is crucial for

\*Address all correspondence to: Ota Samek, E-mail: [osamek@isibrno.cz](mailto:osamek@isibrno.cz)

understanding the processes involved in cells embedded in the biofilm matrix. Such cells are well known to express phenotypes that differ from those of their planktonic counterparts. Moreover, they display specific properties including an increased resistance to chemical agent treatments.<sup>4</sup>

In this study, we focused on eliminating the presence of an extracellular matrix so that only “clean” cells are examined using Raman spectroscopy. In order to visualize the volume of extracellular matrix and reveal differences in the internal structure of the biofilm of our samples, a scanning electron microscopy (SEM) technique was used. It is clear that the combination of Raman spectroscopy with SEM can provide a deeper insight into the chemistry and composition of biofilms. Consequently, from Fig. 1, the volume ratio of cells to the extracellular matrix of about 3 to 1 can be estimated. Thus, this means that the contribution of about 25% of the extracellular matrix from examined volume can translate to Raman spectra and, in turn, can significantly influence the Raman spectra of cells.

In order to obtain the Raman spectrum of biofilm-forming cells without the influence of the extracellular matrix, individual bacterial cells must be extracted out of the colony and localized. A single focused laser beam, known as optical tweezers,<sup>11–16</sup> represents an ideal tool for this task because it provides contactless and sterile spatial trapping of living cells for the time of Raman spectrum acquisition. Such a combination of optical tweezers and Raman microspectroscopy is known as Raman tweezers.<sup>12–20</sup> Thus, living microorganisms can be isolated and trapped in liquid media or microchambers on a chip where their metabolic response to surrounding environment can be investigated in a contactless way by Raman microspectroscopy.<sup>21</sup>

Recently, Raman spectroscopy and an optical tweezers instrument was able to measure the Raman spectra of single or multiple individual spores in aqueous solution using single or multiple traps.<sup>22</sup> Single-cell laser-trapping Raman spectroscopy (Raman tweezers) was used as a method for direct, quantitative, *in vivo* lipid profiling of oil-producing microalgae.<sup>23</sup> Avetisyan et al. used laser tweezers Raman spectroscopy to monitor the *in vivo* real-time uptake and conversion of trehalose by single bacterial cells.<sup>24</sup> Moreover, recent reviews provide valuable information on the exciting advance of Raman tweezers in biomedicine to characterize, discriminate, and identify bacteria at the single-cell level.<sup>25,26</sup>

It has been shown in several studies that Raman microspectroscopy is capable of rapid identification and discrimination of biological samples including medically relevant microorganisms (bacteria and yeast). It has been shown that the technique of Raman spectroscopy (including Raman imaging) can be regarded as the method of choice for many studies of mechanisms that regulate biological processes of microorganisms, cells, and biological samples.<sup>27–35</sup> In addition, a reasonably detailed database of Raman fingerprints from common biological samples has been published.<sup>36</sup>

Raman spectroscopy employs a laser beam that is focused with a microscope objective in order to excite and collect Raman scattering from a small volume of the sample, usually less than 1 fL. A typical Raman spectrum from living microorganism contains a wealth of spectral peaks corresponding to unique interatomic vibrations in biomolecules, e.g., nucleic acids, proteins, carbohydrates, and lipids. Such a spectrum serves as a cellular ‘fingerprint’ and a sensitive indicator of the physiological

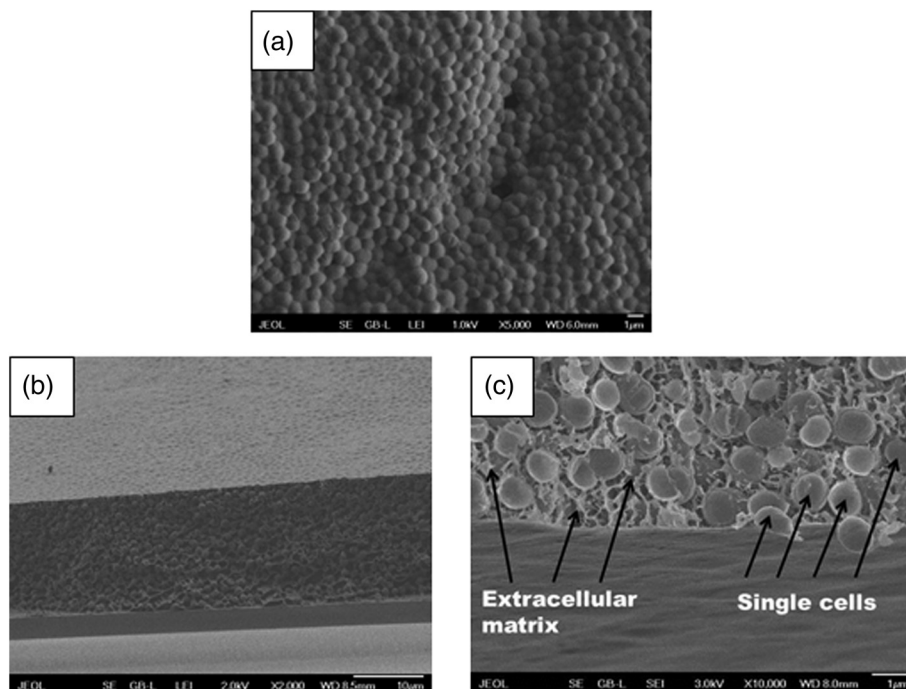


**Fig. 1** Scanning electron microscopy (SEM) images of *Staphylococcus epidermidis* colonies grown on a glass substrate. Biofilm (extracellular matrix or slime) formation is clearly visible throughout the sample filling the space between grape-like clusters of *Staphylococcus* cells. (a) SEM image looking perpendicularly to the surface of a biofilm-forming bacterial colony, (b) SEM image of a fracture (cross section) of the colony, (c) detail of the cells embedded in the extracellular matrix taken from (b). Individual cells and biofilm (extracellular matrix or slime) are denoted by arrows. We estimate that the volume ratio of cells to extracellular matrix is about 3 to 1.

state of the cell.<sup>37</sup> Raman spectra thus enable us to differentiate between different cell types, physiological states, nutrient conditions, and phenotype changes. In principle, Raman spectroscopy requires measurement times on the order of minutes, and sample preparation can be short and extremely economical, e.g., the same substrates, which are used in hospitals for quick infection checks (growing bacteria colonies in Petri dishes), can be directly used.<sup>7</sup>

In order to study how biofilm formation translates into changes in Raman spectra of the cells, the strain pair biofilm-forming *S. epidermidis* and biofilm-negative *S. epidermidis* were used in our study. One expects the matrix composition of bacterial colonies of the biofilm-positive strain to be different from that of the biofilm-negative strain. Thus, one may hope that ability to form the extracellular matrix that makes up the biofilm, also translate into the Raman spectral “fingerprint” of the single bacterial cells, so that it might become feasible to distinguish both positive and negative strains at the level of the single cell. Note that in biofilm-negative strain cells were not experiencing the influence of the extracellular matrix. Thus, their time-course evolution is different from cells living in a biofilm-positive colony. As mentioned above, these cells express different phenotypes.

In this paper, we demonstrate that Raman tweezers are indeed able to distinguish strains of biofilm-forming (biofilm-positive) and biofilm-negative *S. epidermidis* strains with the help of a mathematical method called principal component analysis (PCA).<sup>7</sup> PCA was recently successfully used in the characterization of fetal cells where Jell et al. applied PCA to detect real-time biochemical changes in fetal osteoblast.<sup>38</sup> This work demonstrates the use of PCA to analyze complicated Raman spectra of live cells. It was concluded that PCA analysis can discriminate between cells with small biochemical differences. PCA has also been used for identification of different microorganisms involved in bacterial urinary tract infections employing Raman spectroscopy.<sup>39</sup> PCA was applied to discriminate groups of heat-activated spores based on their Raman spectra.<sup>40</sup> Here, the PCA algorithm was used to determine if minor differences between single untreated spores, cooled heat-activated spores and spores during heat activation can be differentiated based on their individual Raman spectra. Note that PC-loading presentations constitute a valuable tool for estimating the relative contributions from different molecules present in the sample.<sup>38,41</sup>

## 2 Experimental Procedures

### 2.1 Sample Preparation and Experimental Procedures

In order to investigate Raman spectra from single cells (without the influence of an extracellular matrix) selected bacterial cells were directly taken from a bacterial colony using a plastic inoculation loop and diluted in an Eppendorf tube. Consequently, the tube was gently mixed for at least 1 min (on a vortex-mixer) to wash the slime and generate a suspension of single “clean” cells (Fig. 2). It can be noted that extracellular slime is water-soluble and thus could be removed by washing.<sup>42,43</sup> Consequently, a droplet (10  $\mu$ l) of suspension was placed on a microscope coverslip. Thus, we obtained very low concentration of *S. epidermidis* cells ranging between 50 and 70 cells within the microscope field of view (100  $\mu$ m  $\times$  100  $\mu$ m).

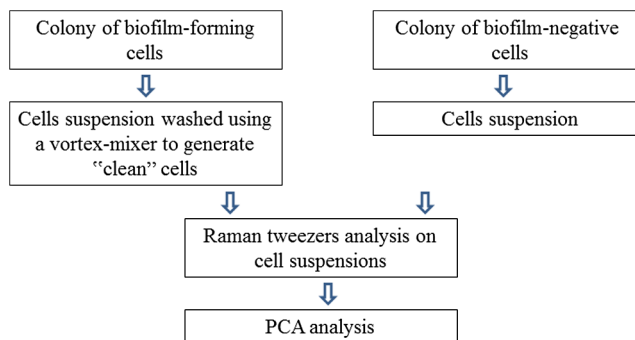


**Fig. 2** Schematic diagram of the experimental procedure. Note that for biofilm-negative cells the “washing step” was skipped.

In the next step, a few (freely moving cells free from extracellular matrix) cells were immediately trapped and analyzed using Raman tweezers. In this way, the contribution from components involved in extracellular matrix, such as, e.g., PIA, was minimized. Consequently, the Raman spectra of bacterial cells were measured. Experiments were carried out using a custom-built experimental system of Raman tweezers.<sup>17,37</sup> Briefly, this combines a Raman microspectrometer with optical tweezers providing spatial confinement of individual bacterial cells (in a form of a single cell or a small cluster) during the Raman spectrum acquisition. The same laser beam is used for optical trapping and Raman spectroscopy. The output beam from a laser (power incident on the sample was about 100 mW,  $\lambda = 785$  nm, Ti:Sapphire, Coherent 899/01, Santa Clara, California) was focused on the sample with a water-immersion objective lens (UPLSAPO 60 $\times$ , NA 1.20, Olympus, Tokyo, Japan).

Note that during the experiments employing the optical tweezers, one living cell suspended in a liquid medium can be immobilized/trapped using the forces generated by a tightly focused laser beam. However, in the liquid with more freely moving bacterial cells, more than one cell which come near the focus could be trapped (this is very difficult to prevent during laser exposition). Estimating that the bacterial cell sizes are less than or comparable to a trapping region of diameter 800 nm, we assume that up to three cells could be trapped and analyzed at the same time. Cells are exposed to the laser light only during spectra acquisition—typically for 10 to 30 s which should give a low enough light dosage not to cause their damage.<sup>44,45</sup>

### 2.2 Raman Spectrum Processing and Analysis

In order to extract quantitative information from the acquired Raman spectra, the statistical classification of the spectra has been carried out in MATLAB. We adopted a Rolling-circle<sup>46</sup> procedure for spectral processing to suppress the wide spectral background, automated subtraction of cosmic ray peaks, and the Savitzky–Golay procedure for subsequent noise filtering. Finally, all the data from all investigated samples were analyzed together using standard PCA algorithms to distinguish the differences between them.

### 2.3 Bacteria Cultivation and Preparation

Well-characterized bacteria—biofilm-positive *S. epidermidis* CCM 7221 and biofilm-negative *S. epidermidis* CCM 4418—were obtained from the Czech Collection of Microorganisms (CCM; Brno, Czech Republic).<sup>47</sup> Before each experiment, the

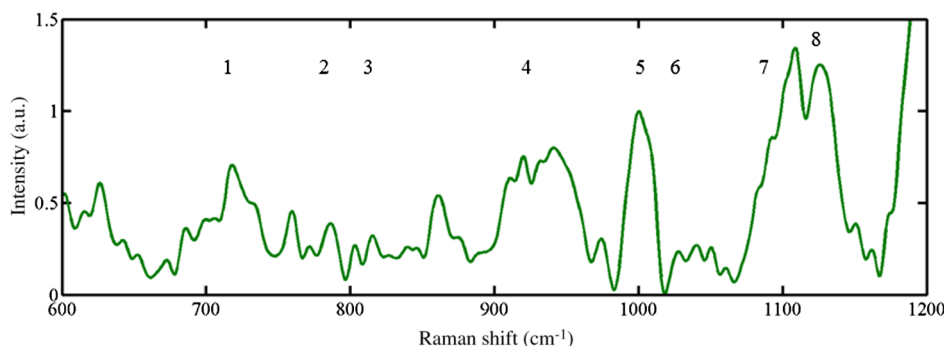


**Fig. 3** Typical Raman spectra of *S. epidermidis* cells (biofilm-forming *S. epidermidis* CCM 7221). The peak numbers are used to identify features in the spectra shown in Table 1.

**Table 1** Summary of prominent peaks/bands observed in the Raman spectra of bacteria, together with suggested assignments of chemical compounds. The peak numbers of this table are used to identify features in the spectra shown in this publication.

Peak No.	Raman feature (cm <sup>-1</sup> )	Suggested assignment <sup>21,27-29</sup>
1	720	Adenine
2	782 to 788	782 cytosine, uracil, thymine (U, C, T) ring breathing 783 phosphoenolpyruvate vibration 783 citric acid vibration 788 phosphor diester O—P—O stretch bond of DNA/RNA
3	813	O—P—O stretch of RNA
4	939 to 954	This band has been correlated with the amount of $\alpha$ -helical structure, skeletal mode of polypeptide backbone (proteins) and C—O—C glycosidic (carbohydrates)
5	1002	Symmetric-ring breathing of phenylalanine amino acid (proteins)
6	1033	C—H in-plane stretch of phenylalanine (proteins)
7	1080 to 1095	1066, 1080 C—C stretch of lipids 1093 C—N stretch of proteins 1095 vibration of phosphor dioxy (PO <sub>2</sub> ) group of deoxyribose sugar (DNA/RNA)
8	1128	1128 C—N stretch of proteins

strains were cultivated on Muller-Hinton's agar (Oxoid, UK) at 37°C overnight. Thus, the colonies used in Raman experiments were approximately 24 h old, and were contained on plastic Petri culture dishes. Colony size was estimated on 1 to 2 mm so that cells could be easily and quickly taken from the colony surface using an inoculation loop.

### 3 Results and Discussion

As mentioned in the experimental section, bacterial cells were taken directly from a bacterial colony. Consequently, they were diluted and analyzed using Raman tweezers in the water droplet. The most prominent features observed in the Raman spectra of bacterial cells shown in Fig. 3 are collected in Table 1.

As can be seen from this summary of spectral features, it is largely the relative abundance of particular biogroups, contained in the fingerprint, which allows identification via, e.g.,

multivariate analysis. We have used the custom-written package to analyze our data using principal component (PC) scores.<sup>41</sup>

In order to differentiate between bacterial species at the level of single investigated cells, we compared the first two PCs obtained from Raman spectra taken from *S. epidermidis* CCM 7221 (biofilm-forming) and *S. epidermidis* CCM 4418 (biofilm-negative). Typical results are shown in Fig. 4. It is seen that in our datasets, the first two PCs are sufficient to distinguish biofilm-forming and biofilm-negative cells with a typical accuracy of about 98% of the total variance. Thus, Raman spectroscopy allows one to evaluate the response of “clean” biofilm-forming cells to cells which do not form biofilm. In this way, the differences in Raman spectra were solely introduced by different phenotypes rather than the extracellular matrix.

As mentioned in Sec. 1, PC-loading presentations target the relative contributions from different molecules present in the sample. Each PC can be further analyzed using the PC-loadings.

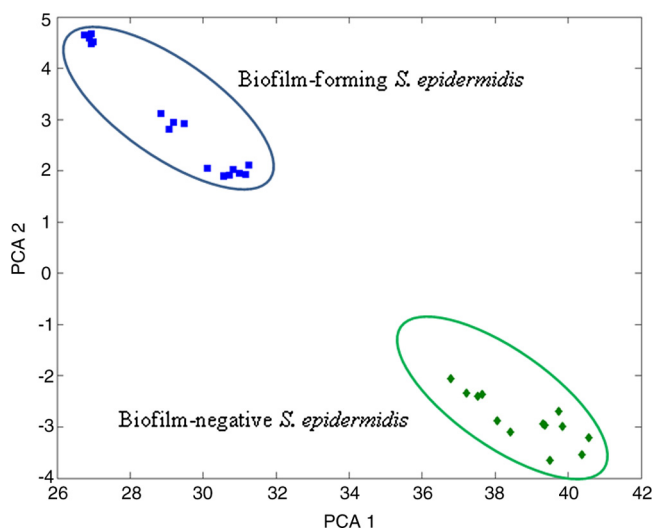


**Fig. 4** Scores or values of the first two principal components PC1 and PC2 obtained from Raman spectra taken from *S. epidermidis* (biofilm-forming, top-left corner) and *S. epidermidis* (biofilm-negative, bottom-right corner).

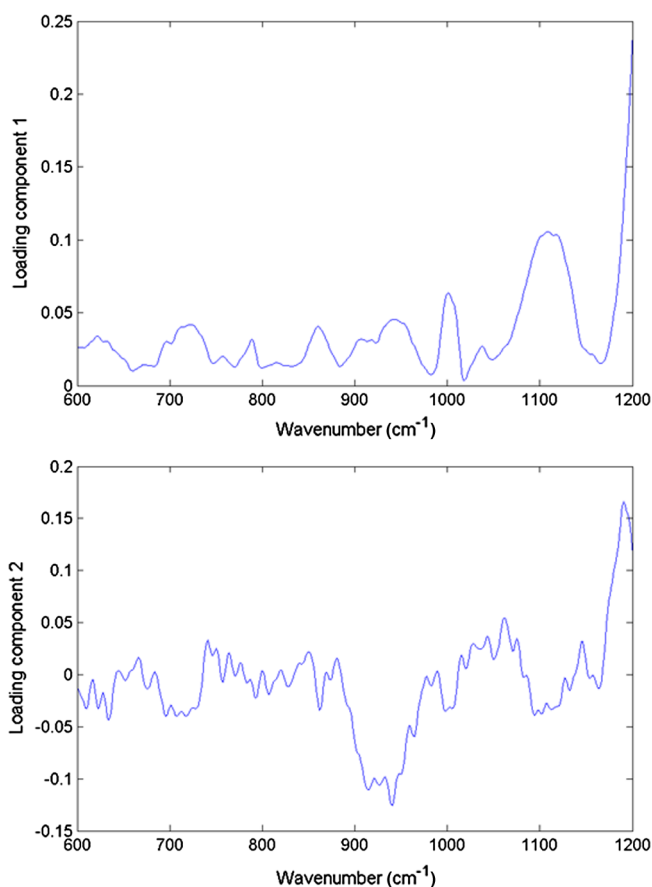


**Fig. 5** Plot of loadings of (a) PC1 and (b) PC2 corresponding to Fig. 4. Different features corresponding to the lipids, proteins, and DNA can be identified as having the largest variability within the data. For example, variances visible in PC2 loading indicates contributions—according to the entries in Table 1—from adenine ( $720\text{ cm}^{-1}$ ), proteins and carbohydrates ( $939\text{ to }954\text{ cm}^{-1}$ ), phenylalanine ( $1002\text{ cm}^{-1}$ ), and at around  $1100\text{ cm}^{-1}$  from lipids, proteins, and DNA. These variances contributed to the clear separation of the two strains shown in Fig. 4.

When these are plotted as a function of Raman shift, they can provide valuable information about the origins of the spectral difference: they can show that Raman features account for the statistical variations. Thus, PC-loadings enable us to follow changes in the Raman spectral pattern for different species. In Fig. 5, the loadings suggest which spectral bands can distinguish biofilm-positive and biofilm-negative strains.

## 4 Conclusions

We combined optical tweezers and Raman microspectroscopy to distinguish—at the single cell level—between two strains of *S. epidermidis* (biofilm-forming and biofilm-negative) in real time and in a contactless way. The biofilm-forming cells were taken directly out of the biofilm colony, diluted, washed from extracellular slime, and investigated by Raman tweezers for less than 30 s. The differences between the spectral Raman fingerprints were analyzed using PCA and just the first two components were sufficient to split the dataset into two distinct groups—*S. epidermidis* biofilm-forming and *S. epidermidis* biofilm-negative.

This shows that a fast, statistically significant analysis using the Raman tweezers is feasible, offering detailed information—in the sense of Raman fingerprints—of the cells expressing different phenotypes.

## Acknowledgments

This research received support from the Czech Science Foundation (GACR P205/11/1687), the Ministry of Health IGA (NS-9678), and the research infrastructure was supported by the Ministry of Education, Youth, and Sports of the Czech Republic (LO1212) together with the European Commission (ALISI No. CZ.1.05/2.1.00/01.0017). Thanks go to Dr. Jana Nebesářová (Biology Centre, ASCR, Czech Republic) for her help during the SEM data gathering.

## References

1. F. Ruzicka et al., “Biofilm detection and the clinical significance of *Staphylococcus epidermidis* isolates,” *Folia Microbiol.* **49**(5), 596–600 (2004).
2. A. I. Spiliopoulou et al., “An extracellular *Staphylococcus epidermidis* polysaccharide: relation to polysaccharide intercellular adhesion and its implication in phagocytosis,” *BMC Microbiol.* **12**, 76 (2012).
3. C. Vuong et al., “Crucial role for exopolysaccharide modification in bacterial biofilm formation, immune evasion, and virulence,” *J. Biol. Chem.* **279**(52), 54881–54886 (2004).
4. A. Bridier et al., “Resistance of bacterial biofilms to disinfectants: a review,” *Biofouling* **27**(9), 1017–1032 (2011).
5. N. K. Karamanos et al., “Identity of macromolecules present in the extracellular slime layer of *Staphylococcus epidermidis*,” *Biochimie* **77**(3), 217–224 (1995).
6. C. Sandt et al., “Confocal Raman microspectroscopy as a tool for studying the chemical heterogeneities of biofilms in situ,” *J. Appl. Microbiol.* **103**(5), 1808–1820 (2007).
7. O. Samek, J. F. M. Al-Marashi, and H. H. Telle, “The potential of Raman spectroscopy for the identification of biofilm formation by *Staphylococcus epidermidis*,” *Laser Phys. Lett.* **7**(5), 378–383 (2010).
8. B. D. Beier, R. G. Quivey, and A. J. Berger “Identification of different bacterial species in biofilms using confocal Raman microscopy,” *J. Biomed. Opt.* **15**(6), 066001 (2010).
9. G. D. McEwen, W. Yangzhe, and Z. Anhong, “Probing nanostructures of bacterial extracellular polymeric substances versus culture time by Raman microspectroscopy and atomic force microscopy,” *Biopolymers* **93**(2), 171–177 (2010).
10. H. C. Flemming and J. Wingender, “The biofilm matrix,” *Nat. Rev. Microbiol.* **8**, 623–633 (2010).

11. A. Ashkin et al., "Observation of single-beam gradient force optical trap for dielectric particles," *Opt. Lett.* **11**(5), 288–290 (1986).
12. D. V. Petrov, "Raman spectroscopy of optically trapped particles," *J. Opt. A* **9**, S139–S156 (2007).
13. A. Jonas and P. Zemanek, "Light at work: the use of optical forces for particle manipulation, sorting, and analysis," *Electrophoresis* **29**(24), 4813–4851 (2008).
14. K. Svoboda and S. M. Block, "Biological applications of optical forces," *Annu. Rev. Biophys. Struct.* **23**, 247–285 (1994).
15. K. C. Neuman and S. M. Block, "Optical trapping," *Rev. Sci. Instrum.* **75**(9), 2787–2809 (2004).
16. J. R. Moffitt et al., "Recent advances in optical tweezers," *Annu. Rev. Biochem.* **77**, 205–228 (2008).
17. O. Samek et al., "Raman microspectroscopy of individual algal cells: sensing unsaturation of storage lipids *in vivo*," *Sensors* **10**(9), 8635–8651 (2010).
18. T. J. Moritz et al., "Evaluation of *Escherichia coli* cell response to antibiotic treatment by use of Raman spectroscopy with laser tweezers," *J. Clin. Microbiol.* **48**(11), 4287–4290 (2010).
19. C. Xie et al., "Identification of single bacterial cells in aqueous solution using confocal laser tweezers Raman spectroscopy," *Anal. Chem.* **77**(14), 4390–4397 (2005).
20. W. E. Huang et al., "Shining light on the microbial world the application of Raman microspectroscopy," *Adv. Appl. Microbiol.* **70**, 153–186 (2010).
21. I. Nottingher and L. L. Hench, "Raman microspectroscopy: a noninvasive tool for studies of individual living cells *in vitro*," *Expert Rev. Med. Devices* **3**(2), 215–234 (2006).
22. L. Kong et al., "Characterization of bacterial spore germination using phase-contrast and fluorescence microscopy, Raman spectroscopy and optical tweezers," *Nat. Protocol* **6**(5), 625–639 (2011).
23. H. Wu et al., "In vivo lipidomics using single-cell Raman spectroscopy," *Proc. Natl. Acad. Sci. U. S. A.* **108**(9), 3809–3814 (2011).
24. A. Avetisyan, J. B. Jensen, and T. Huser, "Monitoring trehalose uptake and conversion by single bacteria using laser tweezers Raman spectroscopy," *Anal. Chem.* **85**(15), 7264–7270 (2013).
25. L. Ashton et al., "Raman spectroscopy: lighting up the future of microbial identification," *Future Microbiol.* **6**(9), 991–997 (2011).
26. D. J. Stevenson, F. Gunn-Moore, and K. Dholakia, "Light forces the pace: optical manipulation for biophotonics," *J. Biomed. Opt.* **15**(4), 041503 (2010).
27. K. Maquelin et al., "Identification of medically relevant microorganisms by vibrational spectroscopy," *J. Microbiol. Methods* **51**(3), 255–271 (2002).
28. J. De Gelder et al., "Raman spectroscopic study of bacterial endospores," *Anal. Bioanal. Chem.* **389**(7–8), 2143–2151 (2007).
29. J. De Gelder et al., "Methods for extracting biochemical information from bacterial Raman spectra: focus on a group of structurally similar biomolecules—fatty acids," *Anal. Chim. Acta* **603**(2), 167–175 (2007).
30. O. Samek et al., "Raman spectroscopy for rapid discrimination of *Staphylococcus epidermidis* clones related to medical device-associated infections," *Laser Phys. Lett.* **5**(6), 465–470 (2008).
31. S. A. Strota et al., "Single bacteria identification by Raman spectroscopy," *J. Biomed. Opt.* **19**(11), 111610 (2014).
32. I. Espagnon et al., "Direct identification of clinically relevant bacterial and yeast microcolonies and macrocolonies on solid culture media by Raman spectroscopy," *J. Biomed. Opt.* **19**(2), 027004 (2014).
33. R. Tuma, "Raman spectroscopy of proteins: from peptides to large assemblies," *J. Raman Spectrosc.* **36**(4), 307–319 (2005).
34. I. Nottingher, "Raman spectroscopy cell-based biosensors," *Sensors* **7**(8), 1343–1358 (2007).
35. A. Harz, P. Rösch, and J. Popp, "Vibrational spectroscopy—a powerful tool for the rapid identification of microbial cells at the single-cell level," *Cytometry Part A* **75A**(2), 104–113 (2009).
36. J. De Gelder et al., "Reference database of Raman spectra of biological molecules," *J. Raman Spectrosc.* **38**(9), 1133–1147 (2007).
37. S. Bernatová et al., "Following the mechanisms of bacteriostatic versus bactericidal action using Raman spectroscopy," *Molecules* **18**(11), 13188–13199 (2013).
38. G. Jell et al., "Bioactive glass-induced osteoblast differentiation: a noninvasive spectroscopic study," *J. Biomed. Mater. Res. A* **86**(1), 31–40 (2008).
39. F. S. de Siqueira e Oliveira, H. E. Giana, and L. Silveira Jr., "Discrimination of selected species of pathogenic bacteria using near-infrared Raman spectroscopy and principal components analysis," *J. Biomed. Opt.* **17**(10), 107004 (2012).
40. P. Zhang, P. Setlow, and Y. Li, "Characterization of single heat-activated *Bacillus* spores using laser tweezers Raman spectroscopy," *Opt. Express* **17**(19), 16480–16491 (2009).
41. O. Samek et al., "*Candida parapsilosis* biofilm identification by Raman spectroscopy," *Int. J. Mol. Sci.* **15**(12), 23924–23935 (2014).
42. M. Herrmann and G. Peters, "Catheter-associated infections caused by coagulase-negative Staphylococci," in *Catheter-Related Infections*, H. Seifert, B. Jansen, and B. M. Farr, eds., pp. 79–109, Marcel Dekker, Inc., New York (1997).
43. P. Kotilainen et al., "Immunochemical analysis of the extracellular slime substance of *Staphylococcus epidermidis*," *Eur. J. Clin. Microbiol. Infect. Dis.* **9**(4), 262–270 (1990).
44. M. Ericsson et al., "Sorting out bacterial viability with optical tweezers," *J. Bacteriol.* **182**(19), 5551–5555 (2000).
45. Z. Pilát et al., "Optical trapping of microalgae at 735–1064 nm: photo-damage assessment," *J. Photochem. Photobiol. B* **121**, 27–31 (2013).
46. N. N. Brandt et al., "Optimization of the rolling-circle filter for Raman background subtraction," *Appl. Spectrosc.* **60**(3), 288–293 (2006).
47. F. Ružička et al., "Capillary isoelectric focusing—useful tool for detection of the biofilm formation in *Staphylococcus epidermidis*," *J. Microbiol. Methods* **68**(3), 530–535 (2007).

Biographies of the authors are not available.